Observations of Storm-time [0]/[N2] Depletion and Thermospheric wind Perturbations using Ground-based Optical Instruments in Alaska during April 4-6, 2010

John Elliott[1], Mark Conde[1], and Jim Hecht[2]. [1]Geophysical Institute, [2]Aerospace Corporation

Motivation

The onset of geomagnetic storms are observed to coincide with large depletions of $[O]/[N_2]$ in the F region thermosphere. Current literature suggests the mechanism for depletion is as follows:

* Joule and particle heating drives strong upwelling in the lower thermosphere near the auroral oval.
* Nitrogen rich (relatively oxygen depleted) air is locally and persistently transported vertically to the F region.
* Neutral winds in the F region disperse nitrogen rich air with predominantly horizontal transport.
* As a result, large geographic regions occur where the column $[O]/[N_2]$ ratio is reduced.

Both theory and observation provide evidence for this well understood mechanism (Burns et al., 1991; Bharti et al., 2018; Craven et al., 1994; Zhang et al., 2004). In contrast to the aforementioned upwelling paradigm, the geomagnetic storm starting April 5, 2010 is one of several observed storms that does not have strong persistent vertical flows, but measurements show a storm time depletion of $[O]/[N_2]$.

We examine observational data collected during the storm over Alaska and offer a complimentary data-driven mechanism by which the depletion is occurring. We illustrate the complex nature of the fluid thermosphere and hypothesize that a vertical gradient in species density and sufficiently turbulent neutral winds exist to create a diffusive mechanism to account for the substantial depression of $[O]/[N_2]$ in the thermosphere.

Remote Sensing Equipment

For the nights surrounding the April 5, 2010 storm ground-based optical instruments at Poker Flat (PKR), Gakona (HRP), and Fort Yukon (FYU), Alaska recorded data. $[O]/[N_2]$ ratio was measured using a pair of four-channel zenith pointed narrow field photometers. Neutral winds were measured using allsky-viewing Fabry-Perot Interferometers, called Scanning Doppler Imagers (SDIs).

The column $[O]/[N_2]$ ratio was estimated from data recorded by photometers viewing the magnetic zeniths above Poker Flat and Fort Yukon in Alaska. Each is equipped with a four-position filter wheel, carrying filters tuned for the 427.8 nm emission from N_2^+, the 630.0 nm and 844.6 nm emissions from atomic oxygen, and the 871.0 nm emission from N_2. These instruments and associated analysis techniques have been described previously by Hecht et al. [10, 11].

The all-sky Fabry-Perot has been described by Conde & Smith [4, 5, 6] and Conde et al. [7]. An all-sky lens maps a zenith-centered field of view spanning around 75^o half-angle in the object space through an interference filter and etalon, with output optics then forming a sharp image onto a 512x512 pixel EMCCD camera. The etalon transmits around 6 interference orders. Techniques described by Conde [5] are used to divide the field of view into 115 sub-regions, and to derive an independent spectrum from each such region. The spectra are fitted as described by Conde [7] to produce line of sight winds. For the April 5 storm the SDI network recorded both 630nm "red" spectra and 558nm "green" spectra.

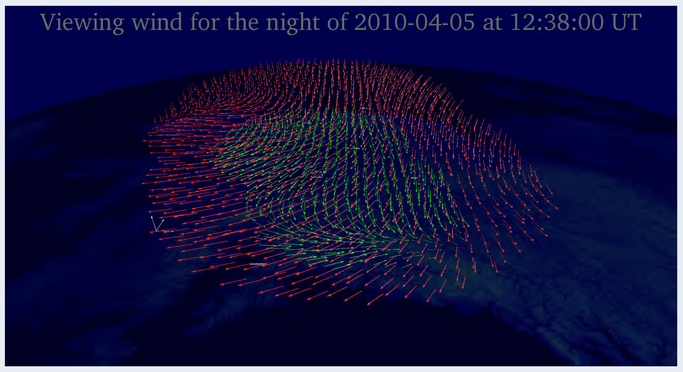

Figure 1: A 3D plot of the neutral winds over Alaska observed by both SDIs on April 5, 2010. Both large and small scale fluid motion are present during the main phase of the storm. The 240km (red) winds exhibit fine structure in the Northwest and the 120km (green) winds in the south. A White reference of 200 m/s exists on the map in southwestern Alaska.

Line of sight winds are then geophysically inverted using techniques evolved from the work of Harding et al. (2015). In total 230 partially overlapped line of sight measurements per channel per time step were mapped to a grid of 25x25km producing 4624 and 1360 inverted vertices per time step for the red and green spectra, respectively (see figure 1 for example). For the process of geophysical inversion red spectra emissions are set to an altitude of 240km and green spectra emissions 120km.

Observations

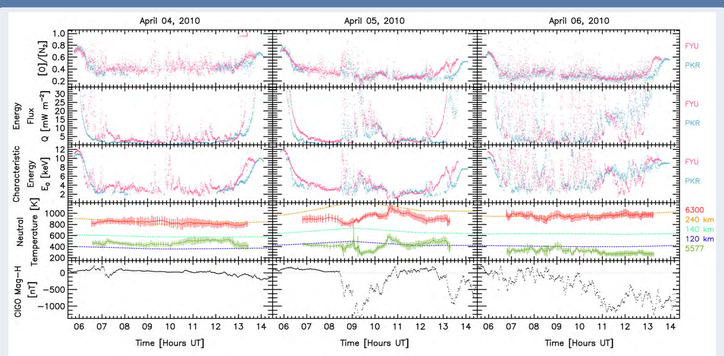

Figure 2: Photometer data products are presented as columns of days and rows of parameters for rows 1-3. SDI mean temperatures are plotted for Poker flat (row 4) and all items are temporally registered with the Alaska-based College magnetometer's H component.

Observations

Figure 3: Each of the top six rows is a stacked time-series of a component of the reconstructed wind at a given latitude, denoted by the vertical axis. Each row is a stacked time-series of a wind component (e.g. red meridional wind). Each column represents one day of time in all components. Latitude scales are maintained across rows, but magnitude scales of wind vary between horizontal and vertical. Barrow, Alaska magnetomter readings are temporally-registered with this data on the last row.

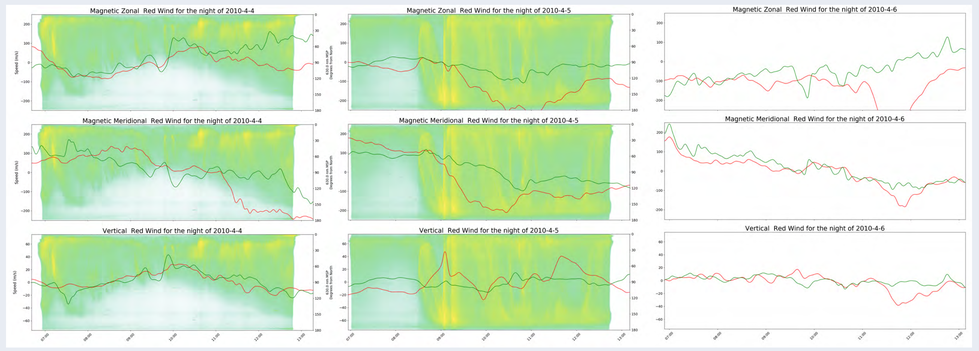

Figure 4: 240km (red) and 120km (green) wind mean speed profiles are presented. Where available Poker Flat meridian keograms are temporally registered in the background indicating auroral activity.

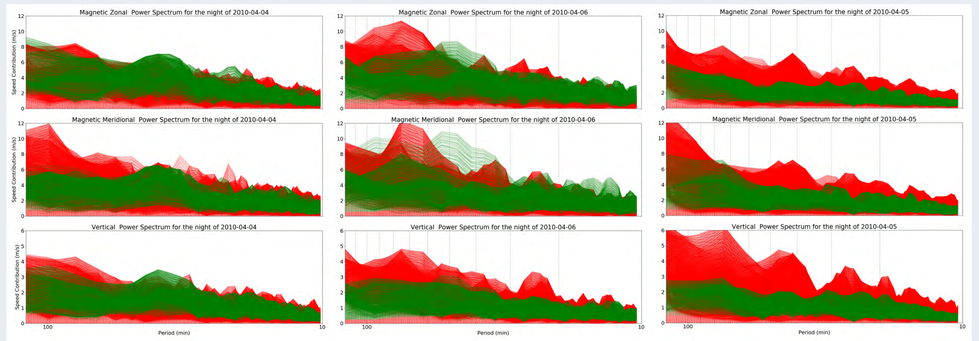

Figure 5: Spectral power has been measured using a Welch filter. Each spatial vertex in the inversion has been plotted as a dashed line of appropriate color. Power spectrum has been converted to units of m/s to show speed contributions.

Results

$[O]/[N_2]$ is inferred for the nights of April 4-6, 2010 (figure 2). A minor (less significant) storm with a well defined initial phase is observed on April 4 (figure 2,column 1). During the night of April 5 the main phase of a large geomagnetic storm is present (figure 2,column 2). Transient behaviour in $[O]/[N_2]$ ratio precedes a sustained depression starting around 0900 April 5. The transient stage is coincident with the depression of the horizontal component of the Alaska-based College magnetometer signalling the initiation of the main phase of the storm, illustrating the response of $[O]/[N_2]$ to the storm.

The winds inferred by geophysical inversion are presented in figures 3,4 along with temporally registered USGS Barrow, Alaska magnetometer horizontal magnetic component measurement (figure 3 column 7). The 0900 onset of the main phase of the April 5 storm is clearly observed in the neutral thermosphere in all latitudes for all wind components (figure 3, column 2). The storm onset drives a significant impulse response to the 240km (red) winds. This response is measurable in the 120km (green) winds, but less markedly at the lower altitude. Most notable is *the absence of sustained persistent upwelling* (figure 3 column 2 row 5, figure 4 column 2 row 2) necessary to deplete the thermosphere of column $[O]/[N_2]$.

Coincident with the onset of the main phase is an initial and dramatic large scale upward surge in the vertical 240km winds. This vertical spike however is short-lived, lasting less than 20 minutes. Following this short impulsive response 240km vertical winds are observed with a large and persistent global ~40 minute period oscillation. Figure 5 (column 2 row 3) shows that the power spectrum is quite enhanced and well structured at 240km altitude on April 5 (when compared to April 4). Additionally near an estimated Brunt–Väisälä frequency of ~10 minutes there is large scale spectral structure indicating the propagation of gravity waves has resulted from the storm-time impulse. Figure 5 also illustrates several other higher frequency structures for this night have both higher amplitude and larger spatial coverage (more vertices registering power at a given frequency), indicating the neutral thermosphere is "ringing" after the onset of the main phase of this storm.

Conclusions

Ground based observations surrounding the April 5, 2010 storm show that:

* The onset of the April 5 storm coincided with the subsequent depletion of $[O]/[N_2]$
* The onset also generated a substantial impulse in the thermospheric neutral winds
* Persistent upwelling was not found in either the 120km or 240km neutral winds
* Oscillatory spatiotemporal structures were formed following the onset of the storm
* The high frequency end of the power spectrum gained amplitude and coherence following the onset of the storm

With the storm-time observation of $[O]/[N_2]$ depletions, "ringing" of the thermosphere by geomagnetic forcing, and the lack of persistent upwelling to accompany the depletion, we conclude that for this event a different mechanism is responsible for the mixing of constituents in the thermosphere. *We suggest that instead of persistent upwelling as the mechanism for $[O]/[N_2]$ depletion, waves that are generated by the storm's impulse into the thermosphere are mixing the lower thermosphere as they propagate, balancing out the existing vertical N_2 gradient.* As is illustrated in figure 3 and figure 5 determination of this mechanism relies on resolving the local structures present in the fluid thermosphere.

References

[1] Bharti, G., Sunil Krishna, M. V., Bag, T., and Jain, P. (2018). Storm time variation of radiative cooling by nitric oxide as observed by TIMED-SABER and GUVI. Journal of Geophysical Research: Space Physics, 123, 1500-1514, doi:10.1002/2017JA024576

[2] Burns, A. G., T. L. Killeen, and R. G. Roble (1991), A Theoretical Study of Thermospheric Composition Perturbations During an Impulsive Geomagnetic Storm, J. Geophys. Res., 96(A8), 14,153–14,167, doi:10.1029/91JA00678.

[3] Burns, A. G., W. Wang, T. L. Killeen, S. C. Solomon, and M. Wiltberger (2006), Vertical variations in the N2 mass mixing ratio during a thermospheric storm that have been simulated using a coupled magnetosphere-ionosphere-thermosphere model, J. Geophys. Res., 111, A11309, doi:10.1029/2006JA011746.

[4] Conde, M., and R. W. Smith, Mapping thermospheric winds in the auroral zone, Geophys. Res. Lett., 22, 3019-3022, 1995. *Conde & Smith 1995*

[5] Conde, M., and R. W. Smith, Phase compensation of a separation scanned, all-sky imaging Fabry-Perot spectrometer for auroral studies, Appl. Opt., 36, 5441-5450, 1997.

[6] Conde, M., and R. W. Smith, Spatial structure in the thermospheric horizontal wind above Poker Flat, Alaska, during solar minimum, J. Geophys. Res., 103, 9449-9472, 1998.

[7] Conde, Craven, Immel, Hoch, Stenbaek-Nielsen, Hallinan, Smith, Olson, Wei Sun, Frank, and Sigwarth, (2001), Assimilated observations of thermospheric winds, the aurora, and ionospheric currents over Alaska, J. Geophys. Res. 106:10493-10508.

[8] Craven, J. D., A. C. Nicholas, L. A. Frank, D. J. Strickland, and T. J. Immel (1994), Variations in the FUV dayglow after intense auroral activity, Geophys. Res. Lett., 21(25), 2793–2796, doi:10.1029/94GL02458.

[9] Harding, B. J., J. J. Makela, and J. W. Meriwether (2015), Estimation of mesoscale thermospheric wind structure using a network of interferometers, J. Geophys. Res. Space Physics, 120, 3928-3940, doi:10.1002/2015JA021025.

[10] Hecht, J. H., A. B. Christensen, D. J. Gutierrez, D. C. Kayser, W. E. Sharp, J. R. Sharber, J. D. Winningham, R. A. Frahm, D. J. Strickland, and D. J. McEwen (1995), Observations of the Neutral Atmosphere Between 100 and 200 km Using ARIA Rocket-Borne and Ground-Based Instruments, J. Geophys. Res., 100(A9), 17,285–17,298, doi:10.1029/95JA00229.

[11] Hecht J.H., D.J. Strickland, and M.G. Conde (2006), The Application of Ground-based Optical Techniques for Inferring Electron Energy Deposition and Composition Change during Auroral Precipitation Events, Journal of Atmospheric and Solar Terrestrial Physics 68:1502-1519.

[12] Zhang, Y., L. J. Paxton, D. Morrison, B. Wolven, H. Kil, C.-I. Meng, S. B. Mende, and T. J. Immel (2004), O/N2 changes during 1–4 October 2002 storms: IMAGE SI-13 and TIMED/GUVI observations, J. Geophys. Res., 109, A10308, doi:10.1029/2004JA010441.